specimens was recorded and reported.

(a) raw image (b) processed image

Figure 4. Test specimen after 6 hours of testing (Gorospe et al. 2019b) (Courtesy of Karla Gorospe)

Early-Age Plastic Shrinkage

Early-age plastic shrinkage was determined in accordance with ASTM C1579 (ASTM 2013a), with modifications based on the experimental procedures undertaken by Gorospe et al. (2019a). In addition, adjustments to the specimen size were also made as a 30 mm thick overlay was laid over a 500 mm x 320 mm x 50 mm concrete restraint element. The test specimen was placed in an environmental chamber with a set operating temperature of 40°C (±2°C) and relative humidity of 15% (± 3%). As shown in Figure 3, two heater fans and a humidifier were used to maintain an evaporation rate of 1 kg/m^2/h. To capture the progression of the early-age cracking, a digital camera was mounted above the chamber. Images of the test specimen were captured at every minute and the total test duration was set to 6 hours.

Figure 5. Measurement of sorptivity (Courtesy of Karla Gorospe)

ImageJ software was used to analyze the captured images for increased accuracy in total crack area quantification. The captured images were processed as an 8-bit image, and the black and white threshold of the image was adjusted to obtain the crack profile of the overlay slab. Figure 4 provides an example of the raw image and the processed image. The crack profiles at every 10-minute intervals, after the first observed crack, were analyzed to determine the crack rate and the total crack area.

Rate of Absorption (Sorptivity)

Sorptivity tests were conducted as per ASTM C1585 (ASTM 2013b). At a specimen age of 365 days, cured cement mortar cylinders with a diameter of 100 mm were cut into 50 mm thick disks and were oven-dried for 24 hours. A silicon coating was applied around each disk specimen and their initial mass was recorded. The specimens were then placed on top of supports in a pan filled with water. Initial rates of absorption were determined based on mass measurements after 1, 4, 9, 16, 25, 49, and 64 minutes of contact with water. Secondary rates of absorption were determined after 1 to 7 days of mass measurements. Figure 5 shows the method of testing.

RESULTS AND DISCUSSION

Compressive Strength

As shown in Figure 6, the replacement of natural sand with glass aggregates results in a reduction in 28-day compressive strength. When comparing with the control specimen (S100G0), the reduction in strength is 15%, 24%, 36%, and 45% for S70G30, S50G50, S30G70, and S0G100, respectively. This strength reduction can be attributed to the weak bond between the cement paste and the smooth glass aggregates, specifically, the glass beads. Similar observations were previously reported by Wright et al. (2014) and Mardani-Aghabaglou et al. (2015).

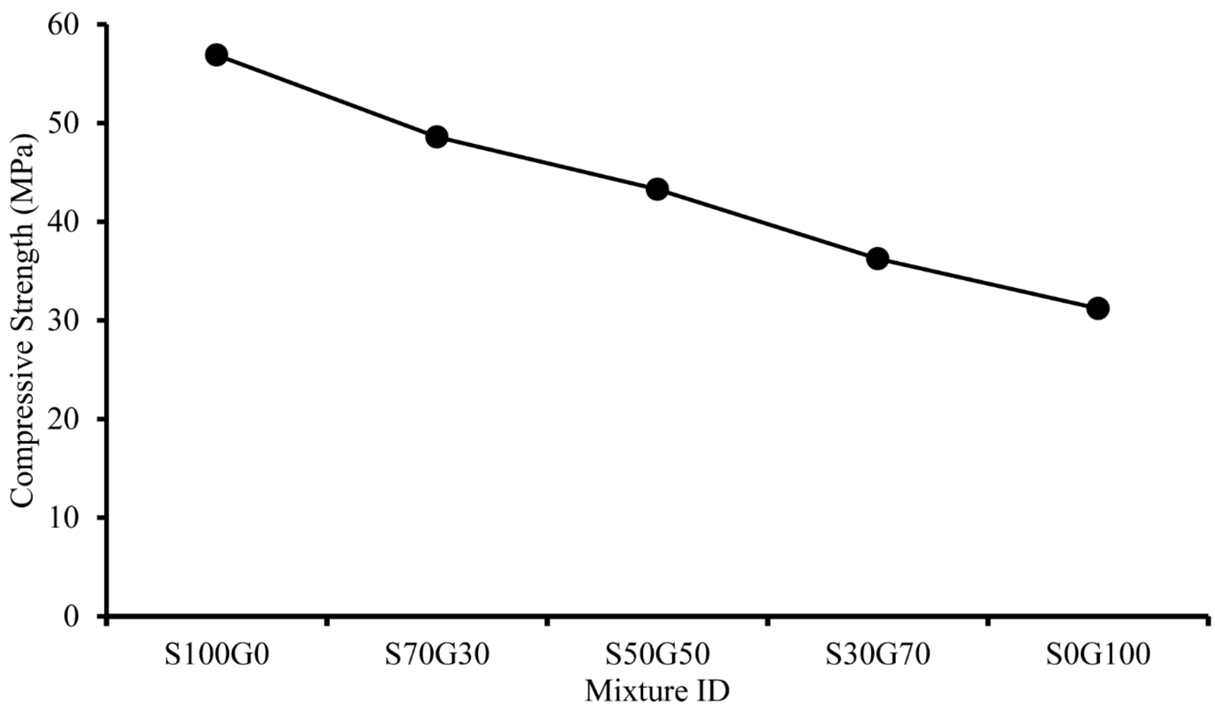

Figure 6. 28-day compressive strength of glass aggregate cement mortars (Courtesy of Karla Gorospe)

Early-Age Plastic Shrinkage

Rapid evaporation of moisture in freshly placed concrete can result in the formation of shallow plastic shrinkage cracks. However, these cracks can ultimately become full-depth cracks after continuous use of the structure and exposure to aggressive environmental conditions. In this study, it was determined that incorporating glass aggregates in cement mortar overlays can significantly reduce cracking due to plastic shrinkage. As shown in Figure 7, a 30% replacement of natural sand with glass can result in an 80% reduction in the total plastic shrinkage crack area. Furthermore, full replacement of sand with glass aggregates results in a 98% crack reduction. The underlying reason for the reduced crack area is the lower absorption rate of the glass aggregates compared to natural sand, which results in more free water for evaporation and thereby delays the drying of the overlay surface. This delay in cracking was quantified in Table 2. In addition, a study by Tan and Du (2013) suggests that glass aggregates improve the overall dimensional stability of cementitious material, which may have led to the better resistance of the glass aggregate mortars to crack formation. Cracking of the cement mortar overlays ensued between 60 and 120 minutes of testing and generally stabilized thereafter.

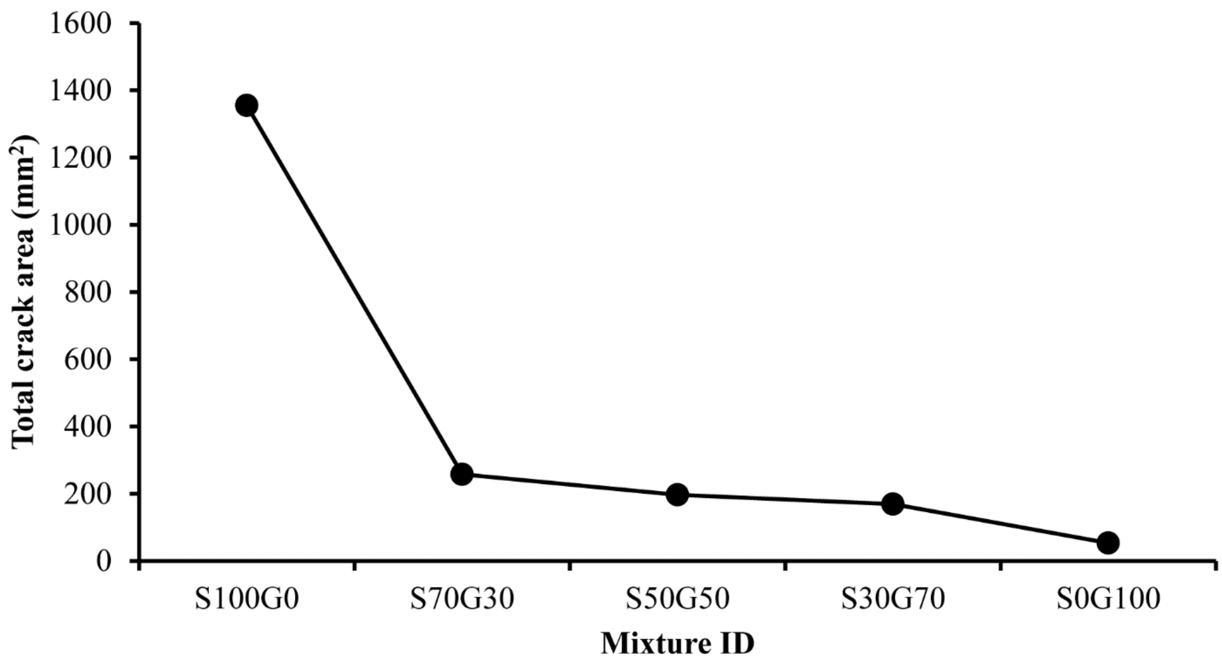

Figure 7. Total plastic shrinkage crack area of glass aggregate cement mortars after 6 hours of testing (Courtesy of Karla Gorospe)

Table 2. Plastic shrinkage crack rate between 60 and 120 minutes of testing (Courtesy of Karla Gorospe)

	S100G0	S70G30	S50G50	S30G70	S0G100
Crack rate (mm^2/min)	22.5	4.4	4.0	3.4	0.5

Rate of Absorption (Sorptivity)

The connectivity of pore networks in cementitious materials can often be evaluated using the initial and secondary rates of absorption (sorptivity). Furthermore, studies have been able to predict the service life of a structure when sorptivity data and exposure conditions are combined (Bentz et al. 2001). Hence, determining the sorptivity of glass aggregate mortars provide much insight into its durability and implications to serviceability. As shown in Figure 8, the sorptivity of cement mortars can be greatly reduced by incorporating glass aggregates. A 31% decrease in initial sorptivity was found when 100% of natural sand was replaced with glass. Similarly, a general reduction in secondary sorptivity was observed with increasing glass aggregate content. The reduction in secondary sorptivity was 8%, 47%, 48%, and 63% for S70G30, S50G50, S30G70, and S0G100, respectively. These results indicate that the glass aggregate mortars are less susceptible to ingress of water and potentially deleterious substances, thereby improving durability and serviceability. According to Wright et al. (2013), glass aggregates in the cement matrix provides an impervious volume that obstructs the passage of water. Moreover, the spherical shape of the glass beads reduces the number of voids in the cement matrix, which also reduces the number of interconnected pores.

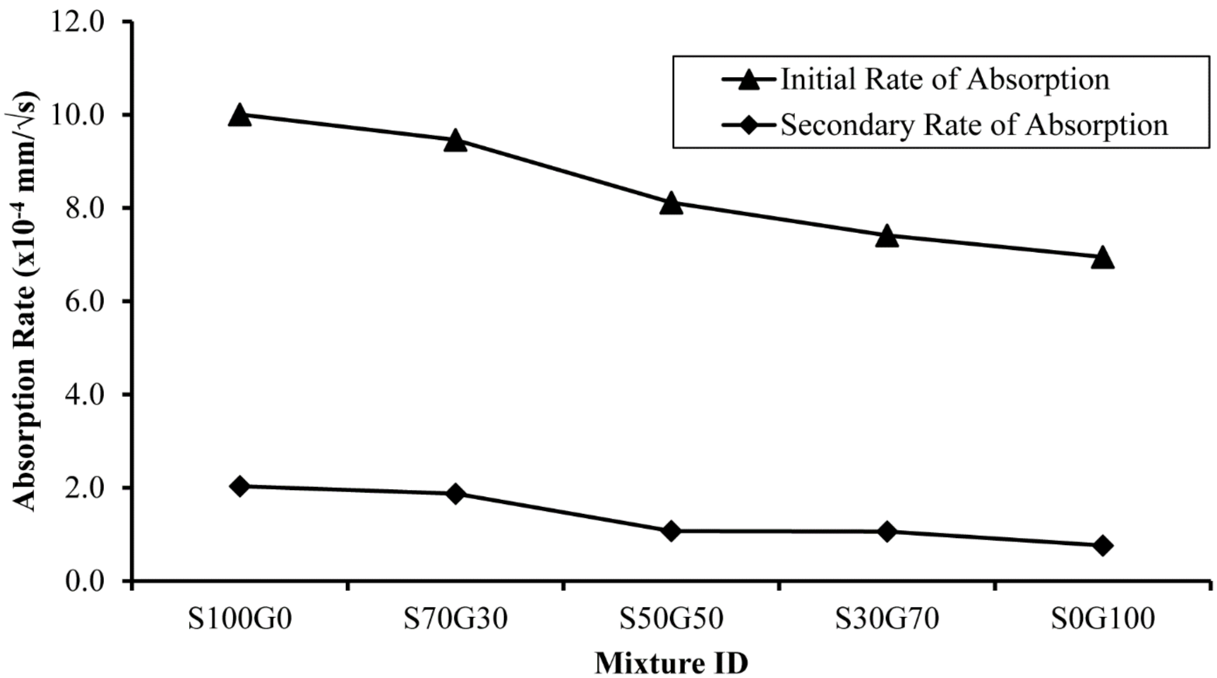

Figure 8. Initial and secondary rates of absorption of glass aggregate cement mortars (Courtesy of Karla Gorospe)

CONCLUSIONS & FUTURE WORK

In this study, the effect of glass aggregates on reducing early-age plastic shrinkage and the rate of absorption was determined for improving the durability of cement mortar overlays. Based on the experimental study conducted, the following conclusions are drawn. It should be noted that the conclusions herein may be limited to the scope of the work.

1. Increasing glass aggregate content reduces overall compressive strength. However, glass aggregates are effective in significantly reducing the formation of cracks associated with early-age plastic shrinkage. At full glass replacement, cracking is reduced by 98%.

2. Initial and secondary rates of absorption are reduced when glass aggregates are used in cement mortars. At full glass replacement, a 31% reduction in initial sorptivity, and a 63% reduction in secondary sorptivity were observed.
3. Exposure of test specimens to a range of environmental conditions should be considered in future studies. Furthermore, to better quantify durability and serviceability, the development of service life prediction models using cracking rates and sorptivity should be considered in future works.

ACKNOWLEDGEMENTS

The authors acknowledge the University of Windsor for the financial support provided to Karla Gorospe in the form of the Queen Elizabeth II Graduate Scholarship in Science and Technology.

REFERENCES

ASTM. 2013a. *Standard test method for evaluating plastic shrinkage cracking of restrained fiber reinforced concrete (using a steel form insert).* ASTM C1579. West Conshohocken, PA: ASTM

ASTM. 2013b. *Standard test method for measurement of rate of absorption of water by hydraulic-cement concretes.* ASTM C1585. West Conshohocken, PA: ASTM

ASTM. 2016. *Standard test method for compressive strength of hydraulic cement mortars (using 2-in. [50-mm] cube specimens).* ASTM C109/ C109M. West Conshohocken, PA: ASTM.

Basheer, L., J. Kropp, and D. Cleland. 2001. "Assessment of the durability of concrete from its permeation properties: A review." Constr. Build. Mater. 15 (2–3): 93–103. https://doi.org/10.1016/S0950-0618(00) 00058-1.

Bentz, D.P., M.A. Ehlen, C.F. Ferraris, and E.J. Garboczi. 2001. "*Sorptivity-based service life predictions for concrete pavements.*" in Proceedings of the 7th International Conference on Concrete Pavements, Orlando, FL. 181-193.

CSA (Canadian Standards Association). 2013. *Cementitious materials used in concrete. CAN/CSA-A3001*. Mississauga, ON: CSA.

De Castro, S., and J. De Brito. 2013. *"Evaluation of the durability of concrete made with crushed glass aggregates."* J. Clean. Prod. 41 (Feb): 7–14. https://doi.org/10.1016/j.jclepro.2012.09.021.

Du H., K.H., Tan. 2013. *"Use of waste glass as sand in mortar: Part II—Alkali-silica reaction and mitigation methods."* Cem. Concr. Comp. 35 (1): 118–126. https://doi.org/10.1016/j.cemconcomp.2012.08.029.

Gorospe, K., E. Booya, H. Ghaednia, and S. Das. 2019, "*Effect of various glass aggregates on the shrinkage and expansion of cement mortar.*" Constr. Build. Mater. 210 (Jun): 301–311. https://doi.org/10.1016/j.conbuildmat.2019.03.192.

Gorospe, K., E. Booya, H. Ghaednia, and S. Das. 2019, "*Strength, Durability, and Thermal Properties of Glass Aggregate Mortars.*" J. Mater. Civ. Eng. 31 (10): 04019231. https://doi.org/10.1061/(ASCE)MT.1943-5533.0002884.

Mardani-Aghabaglou, A., M. Tuyan, and K. Ramyar. 2015. *"Mechanical and durability performance of concrete incorporating fine recycled concrete and glass aggregates."* Mater. Struct. 48 (8): 2629–2640. https:// doi.org/10.1617/s11527-014-0342-3.

Tan, K. H., and H. Du. 2013. *"Use of waste glass as sand in mortar: Part I—Fresh, mechanical and durability properties."* Cem. Concr. Compos. 35 (1): 109–117.

https://doi.org/10.1016/j.cemconcomp.2012 .08.028.
Wright, J. R., C. Cartwright, D. Fura, and F. Rajabipour. 2014. *"Fresh and hardened properties of concrete incorporating recycled glass as 100% sand replacement."* J. Mater. Civ. Eng. 26 (10): 04014073. https://doi.org/10.1061/(ASCE)MT.1943-5533.0000979.

Rehabilitation of Steel I-Beam with Basalt Fiber Reinforced Polymer

Amirreza Bastani[1]; Adeyemi Adesina[2]; Sreekanta Das[3]; and David Lawn[4]

[1]Dept. of Civil and Environmental Engineering, Univ. of Windsor, Windsor, ON, Canada. E-mail: bastani@uwindsor.ca
[2]Dept. of Civil and Environmental Engineering, Univ. of Windsor, Windsor, ON, Canada. E-mail: adesina1@uwindsor.ca
[3]Dept. of Civil and Environmental Engineering, Univ. of Windsor, Windsor, ON, Canada. E-mail: sdas@uwindsor.ca
[4]MEDA Limited, Windsor, ON, Canada. E-mail: dlawn@medagroup.com

ABSTRACT

Deterioration of our infrastructure cannot be totally avoided due to severe conditions to which they are exposed to. A significant number of steel structures, especially bridges, undergoes deterioration due to corrosion as they are situated outdoors and subjected to moisture and other deleterious chemicals. Due to economic and other constraints, replacement of all these deteriorating structures is not feasible. Therefore, their effective rehabilitation is paramount. One of the effective ways to rehabilitate steel structures is with the use of fibre-reinforced polymers (FRP). This paper explores the effectiveness of rehabilitating corroded webs in steel I-shaped beams with unidirectional basalt fibre reinforcement polymer (BFRP) fabric. The structural deficiency was induced to the web of the beam by cutting a circular shaped area out of the web. The section loss was repaired with BFRP fabric using the wet lay-up technique. Overall, seven beams were tested utilizing a 4-point test setup, including a control (undamaged) beam, control corrosion (damaged) beam, and five rehabilitated specimens. Two patterns of rehabilitation were performed by attaching BFRP fabrics in horizontal and vertical orientations. The study concluded that the BFRP fabrics were effective in restoring elastic stiffness, yield load, and ultimate load capacity of rehabilitated beams to that of an undamaged steel beam. The tests also showed that there was a direct correlation between the improvement of structural behaviour and thickness and orientation of the BFRP fabric. Nonlinear finite element analysis was successfully used in this study to determine the optimum pattern of rehabilitation with BFRP fabrics.

1. INTRODUCTION

There are a large number of steel beams in buildings and steel girders and chords in bridges that are structurally deficient and need to be repaired to meet their functional needs. One of the most significant forms of deterioration in steel beams is corrosion of the web. This could be due to various reasons such as an environmental attack, inappropriate maintenance and fatigue damage. A conventional method for rehabilitating steel beams is by attaching additional plates on the damaged area. This has many drawbacks such as increasing the dead load, imposing an additional cost, and creating residual stress and fatigue problems. One of the better rehabilitation methods is the use of fibre reinforced polymer (FRP) materials. FRPs are composite materials consisting of two different parts: matrix and fibre. FRP materials have been widely used as alternative materials for rehabilitating concrete and steel structures. The advantages of FRPs materials are high corrosion resistance, high strength-to-weight ratio, and high fatigue resistance (Al-Saidy et al., 2004). These materials are mostly used in two different forms: prefabricated FRP laminate (plate) and wet lay-up FRP (sheet). Common FRP materials used for rehabilitating structures are glass FRP (GFRP), carbon FRP (CFRP), and basalt FRP (BFRP).

Several studies have been carried out on rehabilitating steel beams using CFRP. Flexural rehabilitation of damaged steel beams using CFRP sheets was conducted by Chen and Das (2009), and Manalo et al. (2016). The studies concluded a slight increase in the stiffness of the rehabilitated beams. In other research, Selvaraj and Madhavan (2017) investigated C channel steel beams rehabilitated with CFRP sheet and found an improvement in failure modes (from lateral torsional buckling to yielding) and flexural moment capacity of the beams. Patnaik et al., (2008) studied flexural and shear strengthening of steel girders with CFRP plates. They showed that by using CFRP plates attached to the web of the girders, shear strength of the steel girders could be increased. El-Sayed et al., (2016) studied the shear behaviour of steel beams strengthened by CFRP and they showed that using layers of diagonal CFRP plates on both sides of the web resulted in increasing the load capacity and decreasing the deformability of beams. Ulger and Okeil (2017) performed tests on thin-walled steel beams rehabilitated with biaxial CFRP sheets and found an increase in shear strength and the load capacity of the retrofitted beams compared to non-retrofitted beams. Attaching CFRP strips (plates) and their alignments on one or both sides of the web was studied by Rigi and Narmashiri (2015) to determine the effect on the shear capacity of the steel beams. They found that diagonal CFRP strips attached on both sides of the web improved shear performance in steel beams more than vertical strips applied in the same manner. However, one of the drawbacks of using this CFRP is the possibility of galvanic corrosion. Thus, various researcher studies have recommended using sufficient thickness of adhesive (e.g. epoxy resin) to avoid direct contact of steel substrate and carbon fabric in steel structures rehabilitated with CFRP (West,2001; Dawood, 2005). Basalt fabric is a relatively new material in construction. This fabric is made of a volcanic rock named Basalt and no additives are added in its production, hence, basalt is a green fabric and more environmentally friendly than carbon. Moreover, there is no concern regarding galvanic corrosion in steel beams retrofitted by BFRP (Jeevanantham et al., 2016). In addition, the cost of basalt fabric is about $1/5^{th}$ of the cost of carbon fabric (Swentek et al., 2016). The other advantages of basalt fabric are its fire resistance, the capability of acoustic insulation, and its immunity to chemical environments (Das and Nizam 2014).

Despite the numerous studies that have been carried out on the rehabilitation of steel beams especially using different fabric polymers in terms of its flexural performance, there exist limited studies on shear performance. Nevertheless, few studies were undertaken to determine the effectiveness of CFRP sheets. However, there exists no research in the open literature about studies performed on the rehabilitation of web corroded steel beams using BFRP fabrics. Hence, this research was designed and carried out to investigate the effectiveness of web corroded steel beams rehabilitated with BFRP fabrics.

2. EXPERIMENTAL PROGRAM

In the current study, the effectiveness of BFRP fabrics for the rehabilitation of simulated web corroded (hereafter web corroded) steel beams was investigated by testing five damaged steel I-beams repaired with different BFRP thicknesses. In addition, two control beam specimens were tested. One of them was a virgin (undamaged) steel beam and the other one was damaged unrepaired steel beam. All the specimens were prepared and tested in the Structural Engineering Laboratory at the University of Windsor.

2.1. Materials

In the current study, a wide flange I beam W150 x 24 (CISC 2014) was selected for preparing all specimens. The tension tests were conducted on eight steel samples (coupons) in accordance with ASTM E8/E8M-15a to determine the mechanical properties of the steel beam and the average results are shown in Table 1. Unidirectional basalt dry fabric (Figure 1) was selected for the rehabilitation of the web corroded steel beams. The specifications of dry basalt fabric prepared by the manufacturer are reported in Table 2. A primer was selected to get a tack-free steel substrate and an epoxy resin was used to impregnate basalt dry fabrics.

Table 1. Properties of steel beam (Courtesy of Amirreza Bastani)

cross section (mm)				Stress (MPa)		Strain (%)		E (GPa)	Poisson's Ratio
Depth	Flange width	Flange thickness	Web thickness	F_y	F_u	ε_y	ε_u		
160	102	10.2	6.6	379	484	0.2	30.0	205	0.3

Table 2. Specifications of unidirectional basalt fabric (Courtesy of Amirreza Bastani)

Fabric type	Fabric Weight (g/m^2)	Fabric thickness (mm)
UD-280-13-60	280	0.45

Structural properties of BFRP composite fabric (dry fabric impregnated by epoxy resin) were determined by performing coupon tests (at least 6 coupons for each test) based on ASTM standards. The average results of modulus of elasticity, ultimate strength and failure strain are shown in Table 3.

Figure 1. Unidirectional basalt fabric(Courtesy of Amirreza Bastani)

2.2. Specimen Preparation

A total of seven steel beam specimens were prepared in this study. Each beam specimen was 1500 mm long. In order to simulate damage (corrosion) for a beam, an area 275 mm long x 100 wide was machined in one side of the beam and on both sides of the web area as shown in Figure 2. The maximum depth of the cut area was 1.65 mm (in one side) as shown in Figure 2a, hence the maximum percentage of the web corrosion was found to be 50% in the mid-height.

Table 3. Structural properties of BFRP composite fabric (Courtesy of Amirreza Bastani)

Property	Orientation	Average value	ASTM Standard
Tensile strength (MPa)	Longitudinal direction	570	D-3039
Tensile modulus (GPa)	Longitudinal direction	25	D-3039
Tensile elongation (%)	Longitudinal direction	2.5	D-3039
Compressive strength (MPa)	Longitudinal direction	350	D-695
Compressive modulus (GPa)	Longitudinal direction	20	D-695
Tensile strength (MPa)	Transverse direction	45	D-3039
Tensile modulus (GPa)	Transverse direction	8	D-3039
Tensile elongation (%)	Transverse direction	0.55	D-3039
Compressive strength (MPa)	Transverse direction	200	D-695
Compressive modulus (GPa)	Transverse direction	14	D-695
In-plane shear strength (MPa)	45° direction	80	D-3518
In-plane shear modulus (GPa)	45° direction	7	D-3518

All the beam specimens were sandblasted to ensure a rough and clean surface. The rehabilitation procedure started by applying a thin layer of primer on the steel surface. The beams were allowed to cure in room temperature for about 24 hours. Then, the dry basalt fabrics were cut in proper lengths. These cut fabrics were impregnated with epoxy resin, and then attached to the web area of the steel beams using a wet lay-up technique. In preparing the rehabilitated beams, attached impregnated basalt fabrics (BFRP) were tied completely to the steel substrate and hence, extra epoxy or any trapped air was released from the composite fabrics. Figure 3 depicts a typical form of a rehabilitation scheme. The rehabilitated beam specimens were cured for seven days before any load application.

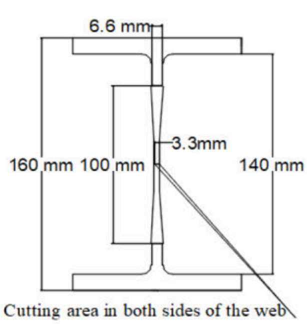

(a) Cross section

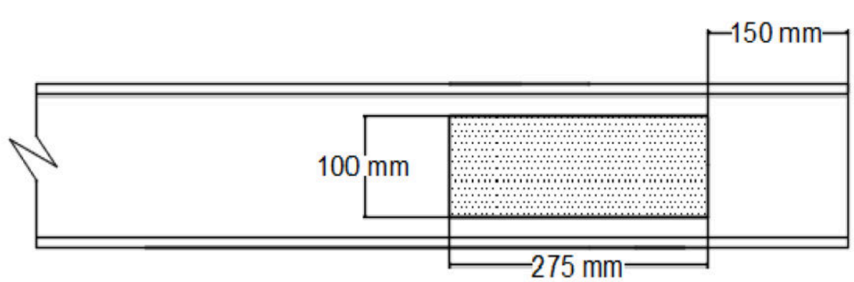

(b) Side view of the beam

Figure 2. Corrosion simulation by machining an area of the web (Courtesy of Amirreza Bastani)